05,07

The features of magnetization processes and phase diagrams of rare-earth ferrimagnets $RFe_{11}TiN_x$ (R = Tm, $x = 0$ and 1) with the $ThMn_{12}$ structure in ultra-high magnetic fields

© V.V. Dorofeev[1,2], N.V. Kostyuchenko[2,3], D.I. Plokhov[1,2,4], I.S. Tereshina[2,5]

[1] Prokhorov Institute of General Physics, Russian Academy of Sciences, Moscow, Russia
[2] Lebedev Physical Institute, Russian Academy of Sciences, Moscow, Russia
[3] Center for Photonics and 2D Materials, Moscow Institute of Physics and Technology, Dolgoprudnyi, Russia
[4] Peoples' Friendship University of Russia named after Patrice Lumumba, Moscow, Russia
[5] Faculty of Physics Lomonosov Moscow State University Moscow, Russia

E-mail: dmitry@plokhov.ru

Received March 16, 2025
Revised March 23, 2025
Accepted March 24, 2025

The full magnetization process of ferrimagnet $TmFe_{11}Ti$ and its nitride $TmFe_{11}TiN_1$ in a magnetic field with induction up to 100 T is investigated. It is shown that the external magnetic field induces reorientation of the iron and thulium sublattices, leading to the implementation of noncollinear and ferromagnetic phases in an ultra-high field. Based on the available experimental data, estimates are given of the effective fields of intersublattice exchange and constants of magnetocrystalline anisotropy. Phase diagrams in the variables „field vs temperature" are obtained.

Keywords: rare earth intermetallics, ultra-high magnetic fields, magnetic phase transitions, full magnetization process.

DOI: 10.61011/PSS.2025.03.60878.52-25

1. Introduction

It is common knowledge that today permanent magnets have extremely wide area of practical application. They are necessary for functioning of all types of devices [1]: power generation devices, including renewable power, electric engines of all types of vehicles, medical equipment, information storage devices etc.

One of the major breakthroughs in the area of design of effective permanent magnets was use of rare-earth intermetallic magnetic materials that started from compound $SmCo_5$ in 1966 [2]. Later, since 1982, the most effective of the magnetically hard materials was intermetallic compound with composition $Nd_2Fe_{14}B$ [3], which remains a leader by some most important characteristics for more than forty years already. However, production and optimization of the highly effective permanent magnets still remains a relevant task for the state-of-the-art technology development.

The most important characteristics, which determine the quality of a strong permanent magnet, are Curie temperature, saturation magnetization and magnetocrystalline anisotropy [4–6]. When the Curie temperature is achieved, the material loses its ferromagnetic properties, therefore it is necessary that its highest possible values provide the possibility to use the magnets under high temperatures (from 400 °C and above), which is critical, for example, for electric engines and power generators.

In the recent decades, rare-earth magnetically hard materials based on iron with common formula $RFe_{11}X$ (R — rare earth element, X — transition element), having tetragonal structure of $ThMn_{12}$ [7,8] type, for example, $RFe_{11}Ti$, have become especially interesting. They are the objects of intensive studies both by experimental methods [13–15] and using the approaches of theoretical modeling [1,9–12,16], which is caused by their outstanding physical properties. They have high Curie temperature T_c, quite high saturation magnetization M_s, and some of them — high value of magnetocrystalline anisotropy constant K_1 [17–19]. These materials are included in the important class of magnetic intermetallic compounds, playing a substantial role in development of highly effective permanent magnets and introduction of new innovation technology [1,20].

The main practical stimulus for the study of such compounds is high cost and strategic importance of rare-earth elements and cobalt, and the need for effective permanent magnets with low content of rare-earth elements [17,19,21]. Compounds $RFe_{11}X$ are characterized by the least ratio of rare earth elements to transition metals compared to other rare-earth intermetallic compounds, in particular, $Nd_2Fe_{14}B$, and their magnetic properties may be considerably im-

proved by introduction of light elements, such as hydrogen or nitrogen [18,22–24].

The main parameters for the rare-earth magnetically hard materials are high energy of magnetic anisotropy, provided by rare-earth ions, in a combination with high magnetization and Curie temperature, related to sublattice of transition metals, usually containing iron and/or cobalt [25,26]. Transition metals contribute insignificantly to anisotropy, because their spin-orbit interaction is low, and their direction of magnetization is determined by interaction with a rare-earth ion. All heavy rare-earth elements (some being rather expensive [27]) have magnetic moments, oriented oppositely to the magnetic moment of the transition metal, which reduces the total magnetization of the material.

Compounds $RFe_{11}Ti$ have an important advantage: due to reduction of rare earth element content (including heavy ones), the percentage share of iron in the composition increases, and, accordingly, magnetization rises per one rare-earth ion. However, decrease in the concentration of rare-earth elements may impact their contribution to the overall magnetic anisotropy. Intermetallic compounds $RFe_{11}Ti$, containing iron and a rare-earth element, represent mostly the materials with pronounced uniaxial magnetic anisotropy provided for by the crystalline structure of the iron sublattice [28,29]. The example of such material is compound $YFe_{11}Ti$, for which the first constant of magnetocrystalline anisotropy is $K_1 = 0.89\,\mathrm{MJ/m^3}$ at room temperature [22,23].

From the research point of view, compounds $RFe_{11}Ti$ cause high interest as objects for the complex modification with the purpose of significant increase of their characteristics and improvement of their properties [13], and also for the detailed understanding of the contribution of rare-earth sublattice, since in contrast to, for example, compounds $R_2Fe_{14}B$ the compounds $RFe_{11}Ti$ have only one rare-earth position, which simplifies the explanation of the behavior and properties of the rare-earth subsystem as such [12,30].

This paper used a model of two-sublattice ferrimagnetic [31,32] to theoretically study the processes of magnetization of single-crystal intermetallic compound $TmFe_{11}Ti$ and its nitride $TmFe_{11}TiN_1$ in magnetic fields up to 100 T, and magnetic phase diagrams of such compounds were obtained in variables „field induction–temperature". The selection of the compound mostly depends on the presence of high-field experimental data for the curves of magnetization in the magnetic field applied both along the light direction (crystallographic c-axis) and in ab-plane [6]. This is especially important, since despite all capabilities of the current experimental technology, every high-field experiment is unique.

The research of the magnetic phase diagrams for the compounds, which may be used as the basis for development of permanent magnets, is relevant since for many practical applications, for example, electric motors, it is important that the material is magnetized gradually, i.e. was in the same magnetic phase in the wide range of external magnetic fields, which is promoted by high values of exchange fields, usually 50−70 T for compositions $RFe_{11}Ti$ [5,6]. From the fundamental point of view and from the point of view of more distant practical applications, it is necessary to study in detail all magnetic phases, which also helps to clarify the key features of behavior of both sublattices: both rare-earth and iron ones.

2. Model of two-sublattice ferrimagnet

Crystalline structure of compounds $RFe_{11}Ti$ is characterized by the presence of one unique position $2a$ (symmetry $4/mmm$) for atom of a rare-earth element and three different positions for iron atoms ($8i$, $8j$ and $8f$). It is important to note that the position $8i$ is occupied by both the iron and the titanium atoms. In case of modification with atoms of light elements (in process of hydrogenation or nitrogenation), hydrogen or nitrogen atoms occupy position $2b$ in the crystalline lattice [5] (Figure 1). This causes noticeable change in the magnetic properties of the material. Atoms of rare-earth elements and iron atoms form two magnetic sublattices, which may either be ordered in a ferromagnetic way (parallel orientation of spins) in case of light rare earth elements, or be ferrimagnetically oriented (anti-parallel orientation of spins) for heavy rare-earth elements.

To study the peculiarities of the magnetization process of the considered compounds in the high and ultra-high magnetic fields, let us use a thermodynamic model of two-sublattice ferrimagnet, which has previously demonstrated its efficiency already [31,32]. Within the model, the problem of finding equilibrium orientations of sublattice magnetization under imposition of the magnetic field by minimization of free energy of the crystal is solved.

The main contributions to the free energy of the crystal are the contribution from action of the external magnetic field to the magnetic moments of rare-earth and iron sublattices, the contribution from the exchange interaction between them, and also the contribution from the availability of the magnetocrystalline anisotropy. The expression for free energy $\mathscr{F}$ calculated per unit of volume may [32] be presented as

$$\mathscr{F} = -\mathbf{M}_F\mathbf{B} - \int_0^{B_R} M_R(T, B'_R)\, dB'_R + W_A. \qquad (1)$$

The first summand here describes the action of the external magnetic field with induction $\mathbf{B}$ at the iron sublattice, and magnetization M_F of iron sublattice is considered to be permanent, not depending on temperature or external magnetic field, in virtue of very strong exchange interaction between the iron atoms. The second summand in the equation (1) determines the energy of interaction of the rare-earth sublattice, which has magnetization M_R, and effective magnetic field B_R. It is important to note that for the compounds in question $M_R < M_F$. Finally, the third summand W_A is the contribution of the magnetocrystalline anisotropy.

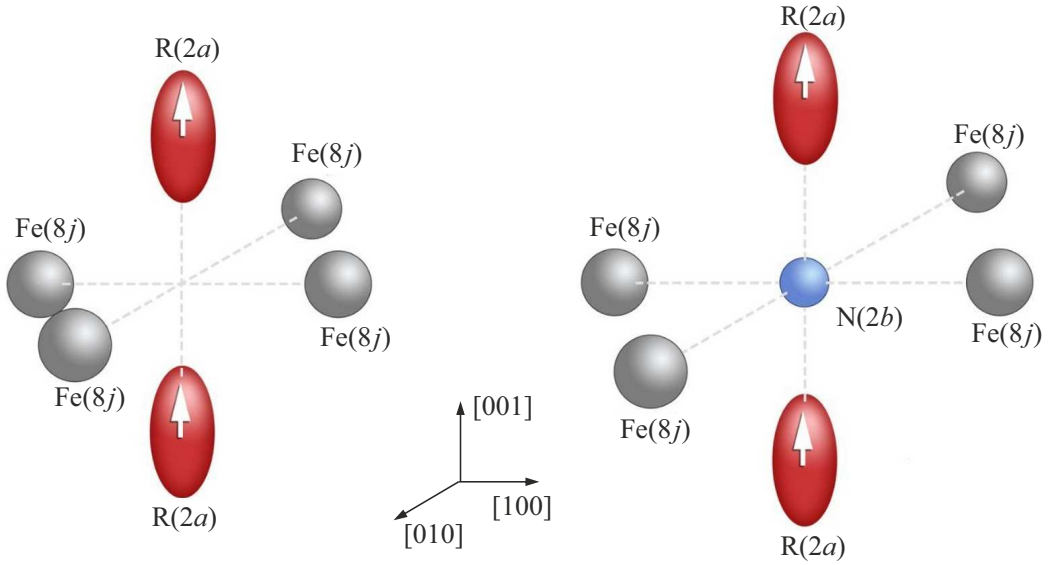

Figure 1. Schematic image of the location of rare-earth element atoms (red), iron atoms (grey), nitrogen atoms (blue) in compounds $RFe_{11}Ti$ and $RFe_{11}TiN_1$ vs. the crystallographic axes: on the left — for the original composition, on the right — for nitride. Arrows inside rare-earth atoms show the direction of their magnetic moments [5].

Since for the rare-earth ions the energy of their exchange interaction with the iron ions is high compared to the energy of the magnetic anisotropy [33], the rare-earth sublattice may be seen as a combination of magnetic elements built along the direction of the effective magnetic field $\mathbf{B_R}$, including the external magnetic field $\mathbf{B}$ and the exchange field $\mathbf{B}_{ex}$:

$$\mathbf{B}_R = \mathbf{B} + \mathbf{B}_{ex} = \mathbf{B} - \mu_0 \lambda \mathbf{M}_F, \tag{2}$$

where μ_0 is magnetic constant, $\lambda > 0$ is exchange interaction constant. It should be noted that the considered model does not take into account the exchange interaction between the ions of the rare-earth sublattice, since in the row of the exchange interactions it is the weakest: R–R ≪ R–Fe ≪ Fe–Fe.

Dependence of magnetization $M_R(T, B_R)$ of the rare-earth sublattice on temperature T and induction B_R of the effective magnetic field, generally speaking, is determined by the exposure of the rare-earth ion to the crystal field. It is commonly known that in the case of the considered intermetallic compounds in the ultra-high magnetic fields the contribution of the crystalline field is not predominant [34]. This conclusion may also be made since the calculations of the magnetization curves $TmFe_{11}Ti$ at $T = 4.2$ K, obtained within the considered theory and under modelling with account of thulium ions exposure to the crystal field [5], yield very close results.

The specified circumstance supports the applicability of a simpler model we use to describe the full magnetization process as a tool for performance of simple and quick estimates of parameters of the studied compounds, including for obtaining the magnetic phase diagrams. Within the two-sublattice ferrimagnetic model the dependence $M_R(T, B_R)$ may be expressed with the help of Brillouin function:

$$M_R(T, B_R) = M_{0R} \cdot B_J\left(\frac{\mu_R B_R}{k_B T}\right), \tag{3}$$

where k_B is Boltzmann constant, M_{0R} is magnetization of the rare-earth sublattice at zero temperature, J is quantum number of total angular momentum of the ground multiplet of the rare-earth ion, and μ_R is value of the rare-earth ion magnetic moment. The ground multiplet of the considered ions Tm^{3+} is $^3H_6$, for which $\mu_R = 7\mu_B$ (μ_B is Bohr magneton).

It is commonly known [35] that the experimentally observed values μ_R in the considered system $RFe_{11}TiN_x$ ($x = 0$ or 1) are close to their theoretical values, specific for a free rare-earth ion R^{3+}, which indicates high degree of localization of $4f$-electrons in the nodes of the rare-earth sublattice and admissibility of using the model of localized magnetic moments in description of the magnetic properties of intermetallic compounds $RFe_{11}Ti$ and their nitrides.

The expression for the anisotropy energy W_A of the crystal in general may be presented in the single-ion approximation, when the iron and rare-earth sublattices make their own contributions. In the case of the considered uniaxial crystals in the expression for the anisotropy energy in the first approximation one may limit oneself to the leading summand

$$W_A(\theta, \varphi) = K_1 \sin^2 \theta, \tag{4}$$

recorded in the system of coordinates, the axes x and z of which are directed accordingly along the crystallographic axes a and c. Note that the constant of anisotropy K_1 is positive.

3. Full magnetization process and magnetic phase diagrams

The study of the full magnetization process comes down to determination of equilibrium orientations of crystal sublattice magnetizations at different values of the external magnetic field and temperature by minimization of the expression (1) for free energy. This paper will consider two cases of orientation of the external magnetic field: along the crystallographic c-axis (longitudinal field) and along the crystallographic a-axis (transversal field).

For the case of the longitudinal field $\mathbf{B} = (0, 0, B)$ we have

$$\frac{\partial \mathscr{F}}{\partial \theta} = M_F B \sin\theta - M_R \frac{\partial B_R}{\partial \theta} + K_1 \sin 2\theta = 0,$$

$$B_R = \sqrt{B^2 + B_{ex}^2 - 2BB_{ex}\cos\theta}, \quad \partial^2\mathscr{F}/\partial\theta^2 > 0, \qquad (5)$$

and for the case of the transverse field $\mathbf{B} = (B, 0, 0)$ we have

$$\frac{\partial \mathscr{F}}{\partial \theta} = -M_F B \cos\theta - M_R \frac{\partial B_R}{\partial \theta} + K_1 \sin 2\theta = 0,$$

$$B_R = \sqrt{B^2 + B_{ex}^2 - 2BB_{ex}\sin\theta}, \quad \partial^2\mathscr{F}/\partial\theta^2 > 0. \qquad (6)$$

To record equations (5) and (6), the system of coordinates introduced above was used, where angle θ specifies the orientation of magnetization of the iron sublattice vs. the crystallographic c-axis. In its turn, the orientation of magnetization of the rare-earth sublattice, specified by angle θ_R, as already mentioned in the model description, is determined by condition $\mathbf{M}_R \parallel \mathbf{B}_R$.

Let us now proceed to the analysis of the peculiarities of the process of full magnetization of ferrimagnetic $TmFe_{11}Ti$ and its nitride $TmFe_{11}TiN_1$. It is feasible to consider separately the cases of the longitudinal and transversal direction of the external magnetic field application. It is also necessary to make a reservation that this paper has no goal to study the details of the magnetization process at low values of external magnetic field induction. When the full magnetization process is considered, it is assumed that the crystal is in the state of the ferrimagnetic saturation already in the zero field.

3.1. Process of full magnetization in longitudinal field

It is easy to see that in the comparatively weak external magnetic field at low temperatures the equation (5) has solutions $\theta = 0$ and $\theta = \pi$, which implement the minimum of free energy (1). Besides, accordingly, $\theta_R = \pi$ and $\theta_R = 0$, i. e. the crystal is in the state of ferrimagnetic ordering. On the contrary, in the very high external magnetic field, ferromagnetic ordering becomes energetically beneficial, when $\theta = 0$ and $\theta_R = 0$. The transition from the ferrimagnetic phase to the ferromagnetic phase takes place via so called angular (noncollinear) intermediate phase [32], where the magnetizations of sublattices deviate from the direction of the applied magnetic field, and $\theta \neq 0$ and $\theta_R \neq 0$.

The boundaries of the noncollinear phase implementation area by magnetic field induction and temperature may be set, if in the equation (5) $\cos\theta = 1$. The detailed analysis shows [32] that there is certain temperature $T_{\max}$, below which there are two critical values of the magnetic field induction, depending on temperature: lower $B_1 = B_1(T)$ and upper $B_2 = B_2(T)$.

If induction B of the external magnetic field does not exceed the lower critical value B_1, the compound is in ferrimagnetic state, when the magnetizations of the rare-earth and iron sublattices are contradirectional, and magnetization of the entire sample is $M_{\text{ferri}} = M_F - M_R$. Upon achievement of the lower critical induction of the field, the second-order phase transition takes place, the noncollinear phase is implemented, where the magnetizations of sublattices deviate from the axis of ferrimagnetic saturation, completing the reorientation towards the forced ferromagnetic ordering, implemented at the field induction exceeding the upper critical value B_2. Sample magnetization reaches the maximum possible value $M_{\text{ferro}} = M_F + M_R$. The described process is a process of full magnetization.

Measurement data [5] of full magnetization curves in the high magnetic fields make it possible to assess the values of the critical fields. Figures 2 and 3 present the experimentally obtained magnetization curves of the considered compound as such and its nitride at temperature 4.2 K in the range of external magnetic fields up to 60 T. Dashed lines reflect the theoretical progress of the magnetization curve in all three implemented phases: horizontal sections are compliant with the ferri- and ferromagnetic phases, and the inclined area — with the noncollinear phase. The points of fracture (in reality — drastic change of the curves inclination) correspond to the critical fields B_1 and B_2.

Using the experiment data, it is possible to quite accurately calculate the constant values of the studied material and its nitride: magnetic moments of iron atoms μ_F and rare-earth atoms μ_R (in Bohr magnetons μ_B), the induction value of the effective exchange field B_{ex} and the constant of the magnetocrystalline anisotropy K_1 (see table). Note that the introduction of a light element atom noticeably changes the material properties. Therefore, the magnetization of the iron sublattice increases, and the intersublattice exchange interaction increases substantially. The seeming decrease of magnetocrystalline anisotropy is explained by the fact that the crystallites of the powder sample of nitride were not previously fully oriented along c-axis of easy magnetization (this is also indicated by the considerable similarity of the magnetization curves in the longitudinal and transverse magnetic fields).

Characteristics of ferrimagnets

Compound	μ_F/μ_B	μ_R/μ_B	B_{ex}, T	K_1, MJ/m^3
$TmFe_{11}Ti$	1.85	7.0	52.7	1.79
$TmFe_{11}TiN_1$	2.00	7.0	71.9	0.71

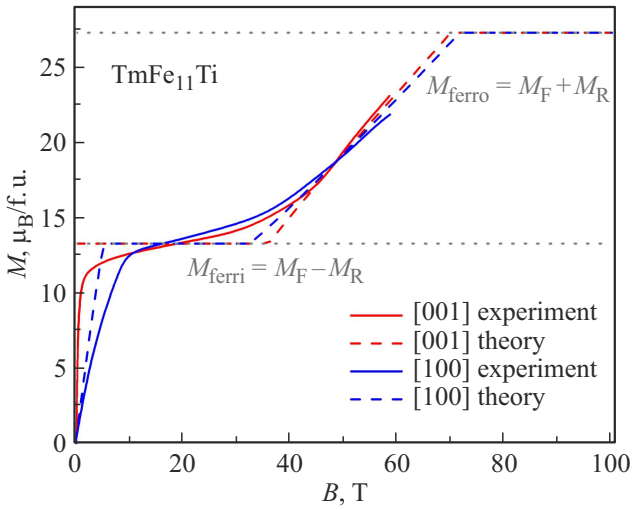

Figure 2. Experimental [5] curves of magnetization (solid lines) of single crystal $TmFe_{11}Ti$, obtained at temperature 4.2 K in magnetic fields, applied along crystallographic axes [0 0 1] and [1 0 0]. Theoretical curves of magnetization (dashed lines) were obtained in this paper within the two-sublattice ferrimagnet model.

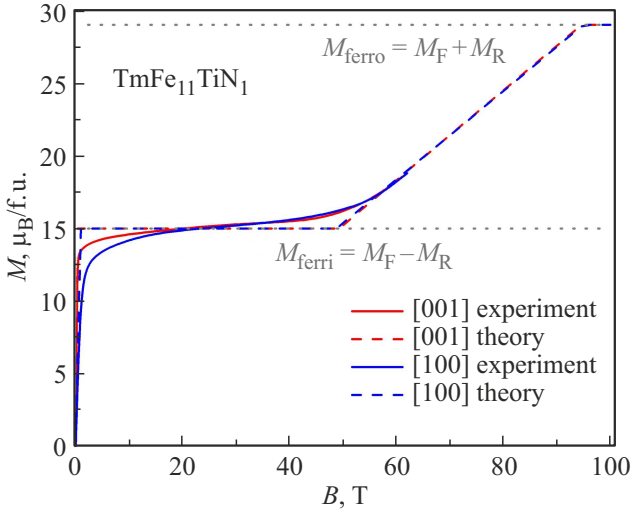

Figure 3. Experimental [5] curves of magnetization (solid lines) of powder oriented sample $TmFe_{11}TiN_1$, obtained at temperature 4.2 K in magnetic fields, applied along crystallographic axes [0 0 1] and [1 0 0]. Theoretical curves of magnetization (dashed lines) were obtained in this paper within the two-sublattice ferrimagnet model.

Analytical expression for values of critical fields B_1 and B_2 may easily be obtained in the limit case $T \to 0$:

$$B_{1,2} = \frac{B_{ex}}{2}\left(1 \mp \frac{M_R}{M_F}\right) - \frac{K_1}{M_F} + \sqrt{\left(\frac{B_{ex}}{2}\left(1 \mp \frac{M_R}{M_F}\right) - \frac{K_1}{M_F}\right)^2 + \frac{2K_1 B_{ex}}{M_F}} \approx B_{ex}\left(1 \mp \frac{M_R}{M_F}\right) \pm \frac{2K_1 M_R}{M_F(M_F \mp M_R)}.$$

For finite temperatures, the numerical solving of equations (5) is necessary. Curves of dependences $B_1(T)$ and $B_2(T)$ are shown in Figure 4. Note that as temperature rises, the lower critical field increases, and the upper field decreases, and they become equal to each other at $T \to T_{max}$. In fact the curves of dependences $B_1(T)$ and $B_2(T)$ represent a phase diagram of the studied compounds $RFe_{11}TiN_x$ ($x = 0$ or 1) in the ultra-high magnetic field in variables „field induction–temperature".

3.2. Process of full magnetization in transversal field

It is evident that in the very high transversal magnetic field (more than 80 T) the state of the forced ferromagnetic ordering is also implemented, when magnetizations of sublattices are built along the direction of the external magnetic field in the basic (ab)-plane, perpendicular to c-axis of easy magnetization. However, the process of full magnetization in the transversal field differs from the process of full magnetization in the longitudinal field.

The main difference is that under the exposure to the relatively weak transverse magnetic field the sample from the state of ferrimagnetic saturation with magnetization $\mathbf{M}_{ferri} \parallel [0\,0\,1]$ changes to the state of the ferrimagnetic saturation with magnetization $\mathbf{M}_{ferri} \parallel [1\,0\,0]$. In process of such reorientation from an easy axis to the basic plane, the magnetizations of the sublattices are noncollinear, therefore the additional angular phase is implemented. Such behavior of the sample is due to the presence of the magnetocrystalline anisotropy, trying „to hold" magnetizations of sublattices in the direction of the easy c-axis.

The further progress of the full magnetization process generally happens as in the case of the longitudinal field: at $B_0 < B < B_1$ the sample is in ferrimagnetic phase, with

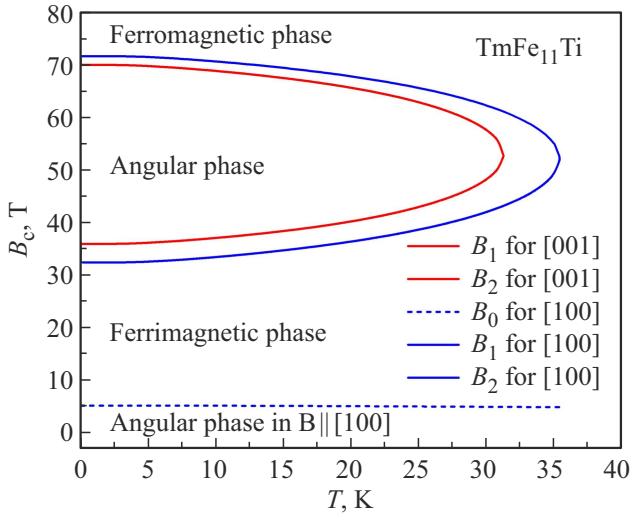

Figure 4. Magnetic phase diagram of single-crystal $TmF_{11}Ti$ in magnetic fields applied along crystallographic axes [0 0 1] and [1 0 0]. The calculation is provided within the theory of two-sublattice ferrimagnet.

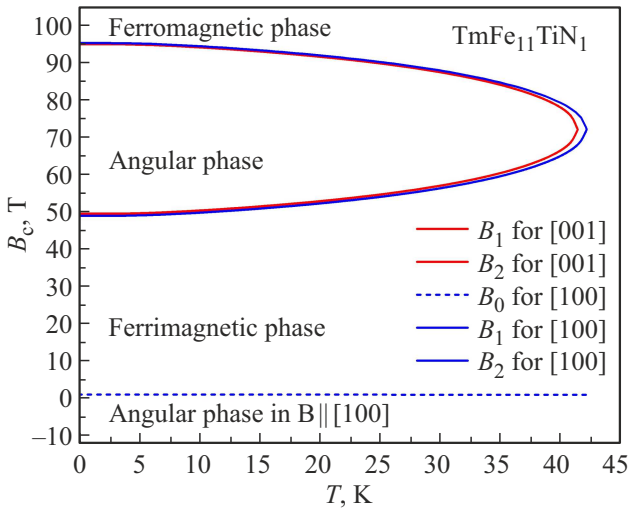

Figure 5. Magnetic phase diagram of powder oriented specimen $TmF_{11}TiN_1$ in magnetic fields applied along crystallographic axes [0 0 1] and [1 0 0]. The calculation is provided within the model of two-sublattice ferrimagnet.

magnetization $M_{\text{ferri}} = M_F - M_R$, directed along the field; at $B_1 < B < B_2$ the noncollinear phase is implemented with deviation of magnetizations of the sublattices from the direction of the external magnetic field; finally, at $B > B_2$ the forced ferromagnetic state is formed, where the sample magnetization reaches the possible limit value $M_{\text{ferro}} = M_F + M_R$, being directed along the external magnetic field. Such similarity of the processes of full magnetization in the longitudinal and transversal fields is quite explainable: as the induction of the external field rises, the contribution to the free energy increases from its interaction with the sublattices, at the same time the relative contribution of the magnetocrystalline anisotropy becomes less and less noticeable. At the same time, due to the presence of anisotropy, the values of critical fields B_1 and B_2 in the case of the transverse field still do not match B_1 and B_2 for the longitudinal field:

$$B_0 = \frac{B_{ex}}{2}\left(1 - \frac{M_R}{M_F}\right) + \frac{K_1}{M_F} - \sqrt{\left(\frac{B_{ex}}{2}\left(1 - \frac{M_R}{M_F}\right) + \frac{K_1}{M_F}\right)^2 - \frac{2K_1 B_{ex}}{M_F}} \approx \frac{2K_1}{M_F - M_R},$$

$$B_{1,2} = \frac{B_{ex}}{2}\left(1 \mp \frac{M_R}{M_F}\right) + \frac{K_1}{M_F} + \sqrt{\left(\frac{B_{ex}}{2}\left(1 \mp \frac{M_R}{M_F}\right) + \frac{K_1}{M_F}\right)^2 - \frac{2K_1 B_{ex}}{M_F}} \approx B_{ex}\left(1 \mp \frac{M_R}{M_F}\right) \mp \frac{2K_1 M_R}{M_F(M_F \mp M_R)}.$$

Temperature dependences $B_0(T)$, $B_1(T)$ and $B_2(T)$ were also obtained by solving the equation (6) using a set of material constants presented in the table. The curves of these dependences are shown in Figures 4 and 5.

4. Conclusion

The main results and conclusions of this paper may be specified as follows: based on the completed measurements of high-field dependences of magnetization of rare-earth ferrimagnetic $TmFe_{11}Ti$ and nitride $TmFe_{11}TiN_1$, the qualitative description is given to the process of full magnetization in ultra-high external magnetic fields, directed both along the easy magnetization axis (crystallographic c-axis), and perpendicularly thereto (ab-plane). The analysis of the experimental magnetization curves made it possible to determine the values of critical fields inducting the reorientation magnetic phase transitions in the considered compounds. Within the model of two-sublattice ferrimagnet it was possible to obtain the estimates of material constants of the studied compounds (value B_{ex} of effective field of intersublattice exchange interaction and constant K_1 of magnetocrystalline anisotropy), and to calculate the magnetic phase diagrams of the studied compounds in variables „field induction–temperature".

The conducted measurements made it possible to experimentally observe the phase transition induced by the magnetic field from the original ferrimagnetic state to the noncollinear state. It was shown that to complete the full magnetization process and to observe the compounds in the ferromagnetic state inducted by the field, the magnetic fields of megagauss range are necessary.

The advantage of the used theoretical model of the full magnetization is its simplicity, and the model made it possible to describe the key peculiarities of this process in the ultra-high magnetic fields and to assess the characteristics of the process and the parameters of the studied compounds. The developed model with minor modifications may be used to study the magnetic properties of various types of rare-earth magnetic materials both in the high and ultra-high magnetic fields.

Funding

This study was conducted within the scientific program of the National Center of Physics and Mathematics (NCPHM), project „Studies in high and ultra-high magnetic fields" (code „NCPHM-7-2325"). The paper of N.V. Kostyuchenko was supported by the Ministry of Science and Higher Education of the Russian Federation (project FSMG-2025-0005). The publication was supported by the Strategic Academic Leadership Program of the Peoples' Friendship University of Russia named after Patrice Lumumba (PFUR).

Conflict of interest

The authors declare that they have no conflict of interest.

References

[1] J.M.D. Coey. Eng. J. **6**, *2*, 119 (2020).
[2] K. Strnat. IEEE Trans. Magn. **6**, *2*, 182 (1970).
[3] J.F. Herbst. Rev. Mod. Phys. **63**, 819 (1991).
[4] A.V. Andreyev, A.N. Bogatkin, N.V. Kudrevatykh, S.S. Sigaev, Y.N. Tarasov. Phys. Met. Metallogr. **68**, *1*, 68 (1989).
[5] I.S. Tereshina, N.V. Kostyuchenko, E.A. Chitrova-Tereshina, Y. Skourski, M. Doerr, I.A. Pelevin, A.K. Zvezdin, M. Paukov, L. Havela, H. Drulis. Sci. Rep. **8**, 3595 (2018).
[6] N.V. Kostyuchenko, I.S. Tereshina, E.A. Tereshina-Chitrova, A.K. Zvezdin. J. Low. Temp. Phys. **200**, 164 (2020).
[7] D.B. De Mooij, K.H.J. Buschow. J. Less Common Metals **136**, *2*, 207 (1988).
[8] C. Xu, L. Wen, A. Pan, L. Zhao, Y. Liu, X. Liao, Y. Pan, X. Zhang. Crystals **14**, *6*, 5071 (2024).
[9] W.Körner, G. Krugel, C. Elsässer. Sci. Rep., **6**, 24686 (2016).
[10] Y. Harashima, K. Terakura, H. Kino, S. Ishibashi, T. Miyake. Phys. Rev. B **92**, 184426 (2015).
[11] R. Skomski, J.M.D. Coey. Scr. Mater. **112**, 3 (2016).
[12] D. Fruchart. In: Magnetic and Superconducting Materials. World Scientific (2000). P. 737.
[13] D.S. Neznakhin, S.V. Andreev, M.A. Semkin, N.V. Selezneva, M.N. Volochaev, A.S. Bolyachkin, N.V. Kudrevatykh, A.S. Volegov. J. Magn. Magn. Mater. **484**, 212 (2019).
[14] I. Ryzhikhin, S. Andreev, M. Semkin, N. Selezneva, A. Volegov, N. Kudrevatykh. J. Phys.: Conf. Series **1389**, 012117 (2019).
[15] B.-P. Hu, H.-S. Li, J.P. Gavigan, J.M.D. Coey. J. Phys.: Condens. Matter **1**, *4*, 755 (1989).
[16] S. Erdmann, T. Klüner, H.I. Sözen. J. Magn. Magn. Mater. **572**, 170645 (2023).
[17] A.M. Gabay, R. Cabassi, S. Fabbrici, F. Albertini, G.C. Hadjipanayis. J. Alloys Compd. **683**, 271 (2016).
[18] X.-D. Zhang, B.-P. Cheng, Y.-C. Yang. Appl. Phys. Lett. **77**, *24*, 4022 (2000).
[19] C. Zhou, K. Sun, F.E. Pinkerton, M.J. Kramer. J. Appl. Phys. **117**, *17*, 17A741 (2015).
[20] O. Gutfleisch, M.A. Willard, E. Brück, C.H. Chen, S.G. Sankar, J.P. Liu. Adv. Mater. **23**, *7*, 821 (2011).
[21] J. Shehu, I. Shetinin. SSRN preprints. https://ssrn.com/abstract=4557924
[22] I.S. Tereshina, P. Gaczyński, V.S. Rusakov, H. Drulis, S.A. Nikitin, W. Suski, N.V. Tristan, T. Palewski. J. Phys.: Condens. Matter **13**, *35*, 8161 (2001).
[23] W. Suski. Handb. Phys. Chem. Rare Earths **22**, 143 (1996).
[24] S.A. Nikitin, I.S. Tereshina, V.N. Verbetsky, A.A. Salamova. J. Alloys Compd. **316**, *1–2*, 46 (2001).
[25] H.-S. Li, J.M.D. Coey. Handb. Magn. Mater. **28**, 87 (2019).
[26] A.A. Makurenkova, M.V. Zhelezny, N.Y. Pankratova, E.S. Kozlyakova, I.S. Tereshina, S.A. Nikitin. Bull. of the Russian Academy of Sciences: Physics **87**, *4*, 420 (2023).
[27] www.compoundchem.com
[28] K.P. Belov, A.K. Zvezdin, A.M. Kadomtseva, R.Z. Levitin. Orientatsionniye perekhody v redkozemelnykh magnetikakh. Nauka, M. (1979). 317 s. (in Russian).
[29] H.C. Herper, K.P. Skokov, S. Ener, P. Thunström. Acta Materialia **242**, 118473 (2023).
[30] C. Abadía, P.A. Algarabel, B. García-Landa, M.R. Ibarra, A. del Moral, N.V. Kudrevatykh, P.E. Markin. J. Phys.: Condens. Matter **10**, *2*, 349 (1998).
[31] N.V. Kostyuchenko, D.I. Plokhov, V.V. Dorofeev, M.D. Kolyadenko, E.N. Syomushkina, A.K. Zvezdin. Inzh. fiz. *5*, 12 (2024). (in Russian).
[32] N.V. Kostyuchenko, D.I. Plokhov, I.S. Tereshina, G.A. Politova, Yu.B. Kudasov, V.V. Platonov, O.M. Surdin, D.A. Maslov, I.S. Strelkov, R.V. Kozabaranov, P.Yu. Katenkov, A.S. Korshunov, I.V. Makarov, A.I. Bykov, A.V. Filippov, E.A. Bychkova, P.B. Repin, V.D. Selemir, A.A. Gorbatsevich, A.K. Zvezdin. ZhETF **166**, *6*, 846 (2024). (in Russian).
[33] V.I. Silantiev, A.I. Popov, R.Z. Levitin, A.K. Zvezdin. ZhETF **78**, *2*, 640 (1980). (in Russian).
[34] C. Piquer, F. Grandjean, O. Isnard, G.J. Long. J. Phys.: Condens. Matter. **18**, *1*, 221 (2006).
[35] I.S. Tereshina. Fizika redkozemelnykh intermetallicheskikh soedineniy, ikh gidridov i nitridov. Izd-vo fiz. f-ta MGU, M. (2020). 232 p. (in Russian).

Translated by M.Verenikina